SAND2022-13307C

Sandia National Laboratories

Sandia National Laboratories is a multimission laboratory managed and operated by National Technology & Engineering Solutions of Sandia, LLC, a wholly owned subsidiary of Honeywell International Inc., for the U.S. Department of Energy's National Nuclear Security Administration under contract DE-NA0003525.

High-Fidelity Retrieval of Instantaneous Line-of-Sight Returns from Nacelle-Mounted Lidar including Supervised Machine Learning

Presentation at 2022 NAWEA/WindTech
Newark, DE, USA

K A Brown
Sandia National Laboratories
T G Herges
Sandia National Laboratories

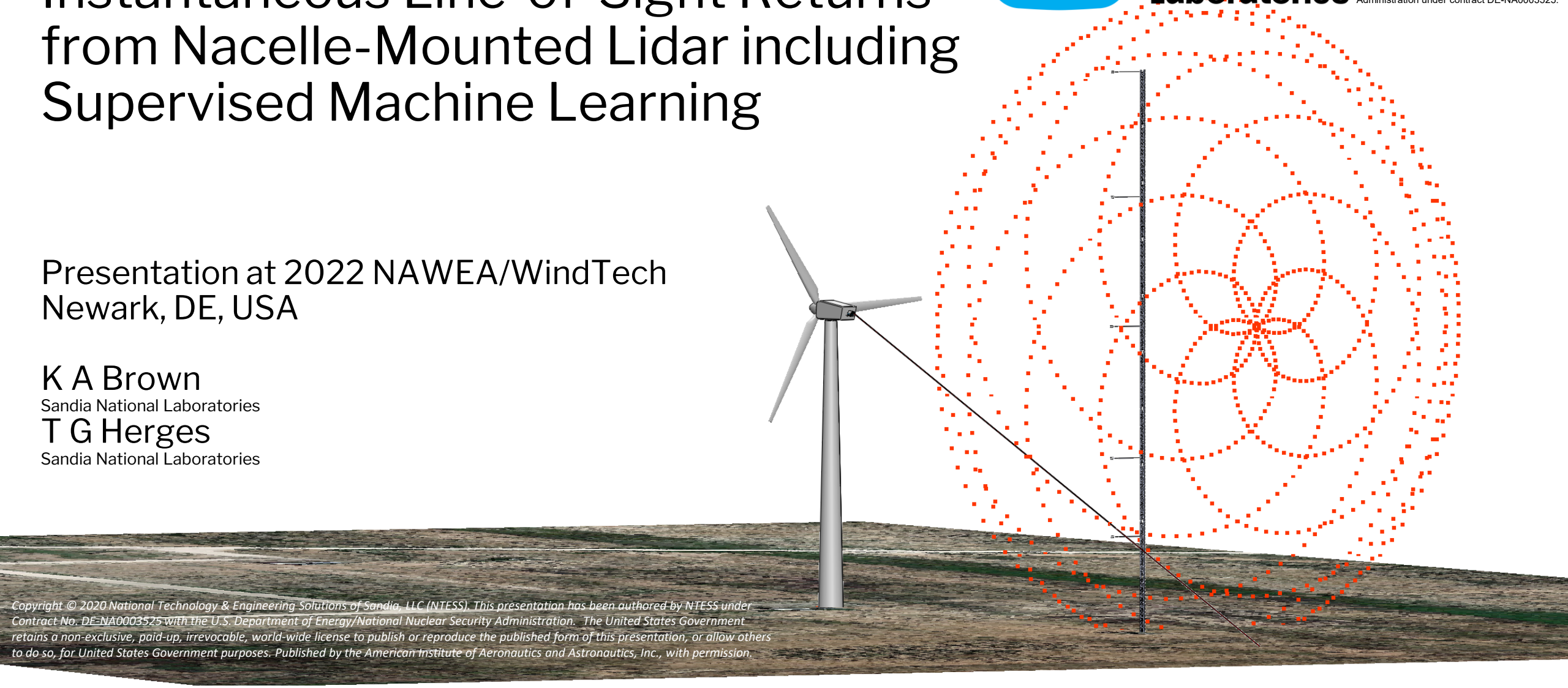

Sandia National Laboratories is a multimission laboratory managed and operated by National Technology & Engineering Solutions of Sandia, LLC, a wholly owned subsidiary of Honeywell International Inc., for the U.S. Department of Energy's National Nuclear Security Administration under contract DE-NA0003525.

Motivation

Why are we talking about lidar processing?

Nacelle-mounted Doppler lidar is relevant for:

- site selection [1, 2]
- power performance testing [3]
- feedforward control [4-6]
- model validation [7, 8]

Instrument error missing from existing validation studies

Uncertainties in lidar-derived data stem from [9, 10]:

1. lidar line-of-sight velocity readings themselves
2. modeling approaches for reconstruction of the velocity vector

Our work focuses on quantification of the first, more fundamental source of lidar uncertainty that is present in all lidar measurements

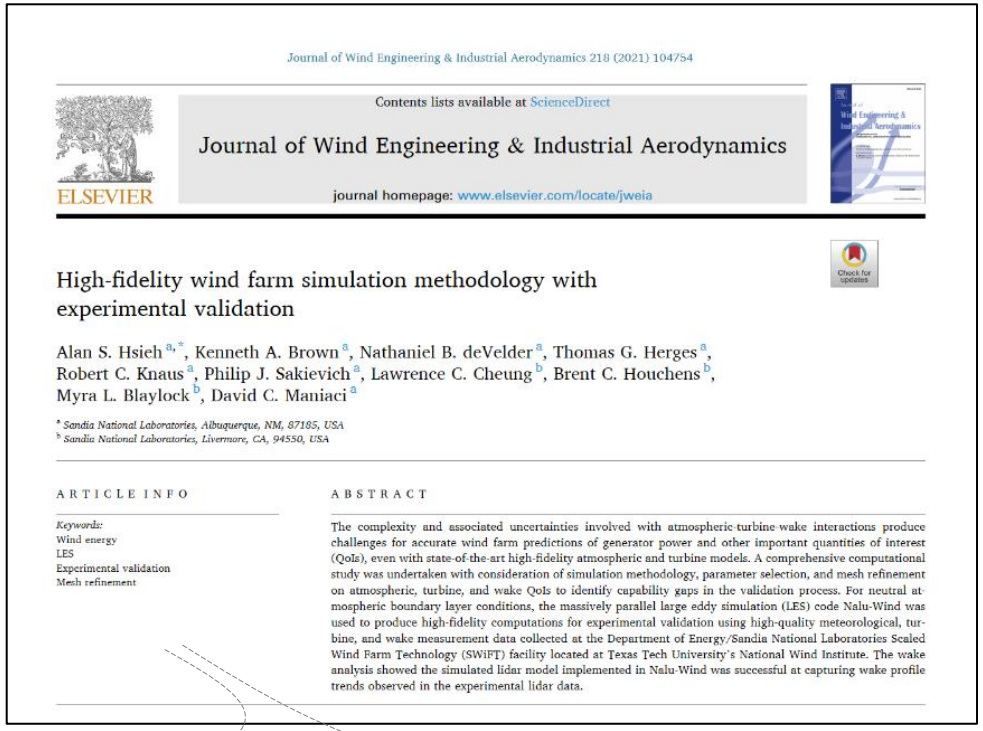

Journal of Wind Engineering & Industrial Aerodynamics 218 (2021) 104754

Contents lists available at ScienceDirect

Journal of Wind Engineering & Industrial Aerodynamics

journal homepage: www.elsevier.com/locate/jweia

ELSEVIER

High-fidelity wind farm simulation methodology with experimental validation

Alan S. Hsieh [a,*], Kenneth A. Brown [a], Nathaniel B. deVelder [a], Thomas G. Herges [a], Robert C. Knaus [a], Philip J. Sakievich [a], Lawrence C. Cheung [b], Brent C. Houchens [b], Myra L. Blaylock [b], David C. Maniaci [a]

[a] Sandia National Laboratories, Albuquerque, NM, 87185, USA
[b] Sandia National Laboratories, Livermore, CA, 94550, USA

ARTICLE INFO

Keywords:
Wind energy
LES
Experimental validation
Mesh refinement

ABSTRACT

The complexity and associated uncertainties involved with atmospheric turbine wake interactions produce challenges for accurate wind farm predictions of generator power and other important quantities of interest (QoIs), even with state-of-the-art high-fidelity atmospheric and turbine models. A comprehensive computational study was undertaken with consideration of simulation methodology, parameter selection, and mesh refinement on atmospheric, turbine, and wake QoIs to identify capability gaps in the validation process. For neutral atmospheric boundary layer conditions, the massively parallel large eddy simulation (LES) code Nalu-Wind was used to produce high-fidelity computations for experimental validation using high-quality meteorological, turbine, and wake measurement data collected at the Department of Energy/Sandia National Laboratories Scaled Wind Farm Technology (SWiFT) facility located at Texas Tech University's National Wind Institute. The wake analysis showed the simulated lidar model implemented in Nalu-Wind was successful at capturing wake profile trends observed in the experimental lidar data.

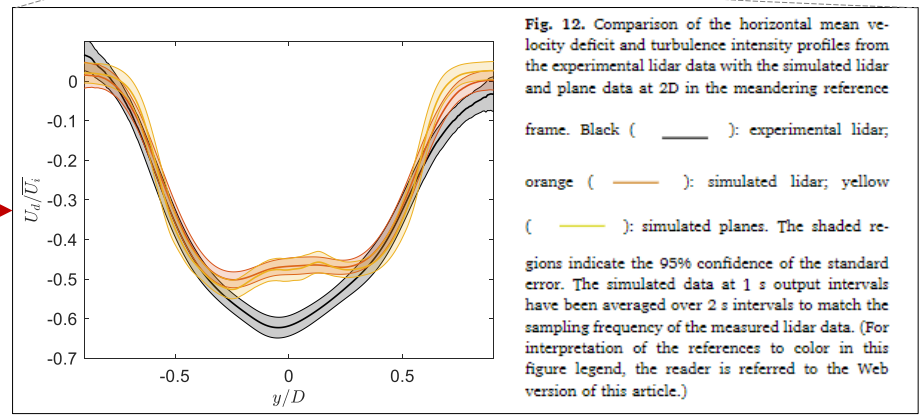

Fig. 12. Comparison of the horizontal mean velocity deficit and turbulence intensity profiles from the experimental lidar data with the simulated lidar and plane data at 2D in the meandering reference frame. Black (____): experimental lidar; orange (____): simulated lidar; yellow (____): simulated planes. The shaded regions indicate the 95% confidence of the standard error. The simulated data at 1 *s* output intervals have been averaged over 2 *s* intervals to match the sampling frequency of the measured lidar data. (For interpretation of the references to color in this figure legend, the reader is referred to the Web version of this article.)

Problem

What is still left to do?

Uncertainty in line-of-sight velocity stems from:

a) Imperfect control of beam position [5, 11]

b) Imperfect point resolution due to beamwise averaging [5, 12-15]

- Modern lidars show biases $\sim\leq$ 0.2-m/s and std. dev. $\sim\leq$ 0.20-m/s depending mostly on the inhomogeneities in the flow [21]
- Solid-body returns (previous work for airborne case in [19]) also stem from beamwise averaging

c) Imperfect instrument (instrument/shot noise) [5, 16, 17]

- Low carrier-to-noise ratio (CNR) found in fast-scanning (i.e., ~500 Hz) continuous-wave (CW) lidar [18]

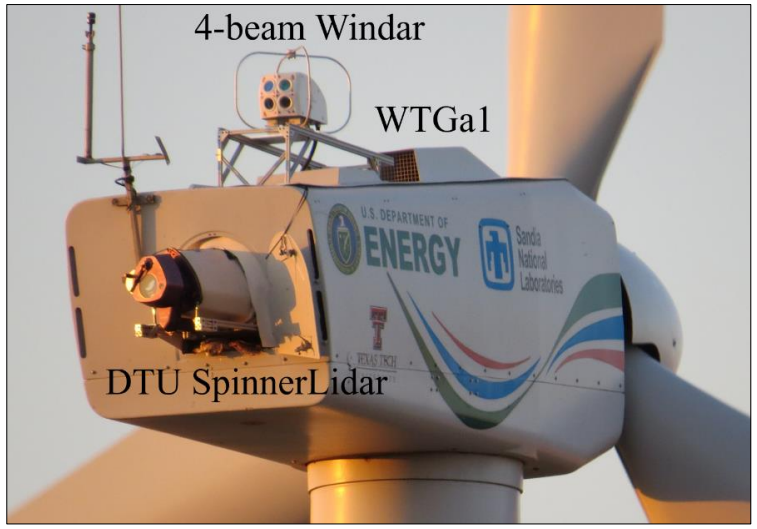

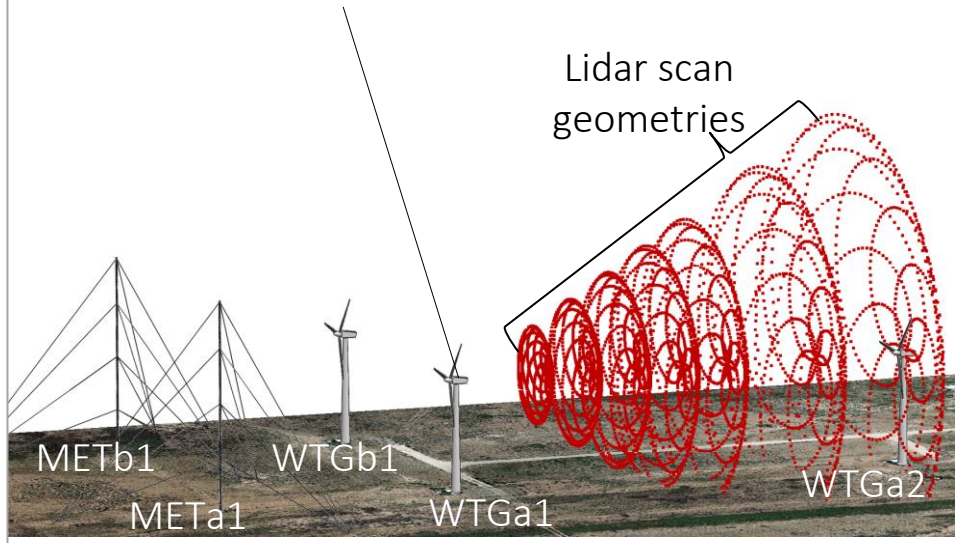

Rendering of the SWiFT facility in Lubbock, Texas, USA with image of the rear-mounted DTU SpinnerLidar

Solid interference and amplitude noise are largely unquantified error sources and ones that cannot be determined *a priori;* these errors must be handled by the retrieval process.

Experimental Method

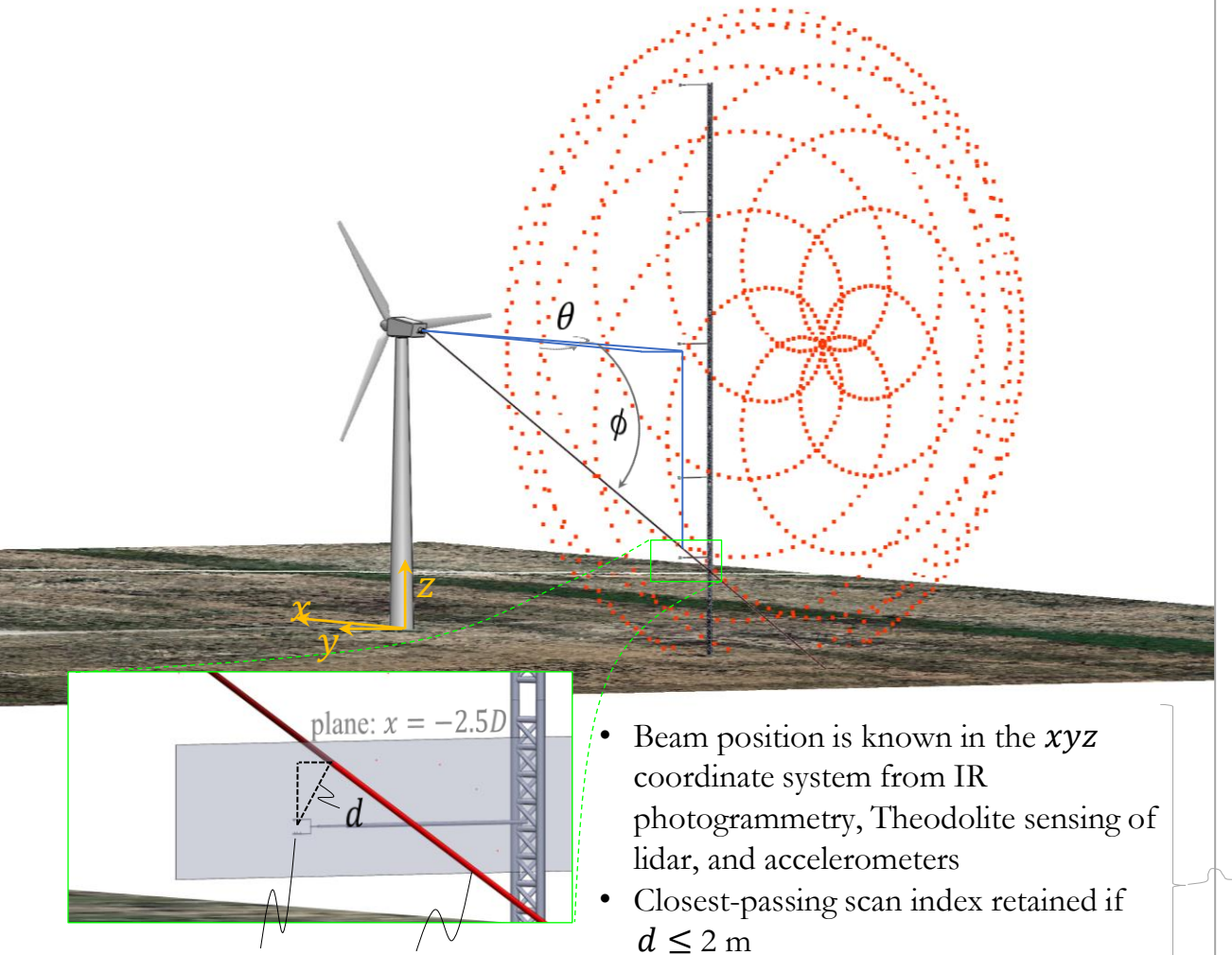

- Beam position is known in the xyz coordinate system from IR photogrammetry, Theodolite sensing of lidar, and accelerometers
- Closest-passing scan index retained if $d \leq 2$ m
- Sonic data interpolated in time to the moment when beam passed within 2 m

Facility

- Scaled Wind Farm Technology (SWiFT) facility
- Data from 2016-2017 wake steering campaign[22]

Ultrasonic Anemometers

- Five SATI Series 'A' style probe sonic anemometers from ATI Technologies, Inc. (accuracy ± 0.01 m/s)

Laser Anemometer (Lidar)

- Continuous-wave (CW) DTU SpinnerLidar [3] rear-mounted on WTGa1 (rotated 180°)
- A rosette pattern is completed every 2-4 s and consist of 984-1968 measurement locations

Pre-Processing

- Filter to 69 bins for inflow and 6 bins for wake
- Spatio-temporal syncing
- Projection of velocity components:

$$u_{sonic}^{los} = [\cos(\theta)\cos(\phi) \quad \sin(\theta)\cos(\phi) \quad \sin(\phi)] \begin{pmatrix} u_{sonic} \\ v_{sonic} \\ w_{sonic} \end{pmatrix}$$

Retrieval Techniques

Technique 1: conventional thresholding (CT) [16, 18]

$$s_{th.} = s - \mu_{noise} - \sigma_{noise}\, n_\sigma$$

- $s_{th.}$: Thresholded spectrum
- s: Raw spectrum
- μ_{noise}: Mean noise level
- σ_{noise}: Std. dev. of noise level
- n_σ: Number of σ_{noise} above the noise floor of the desired threshold level

These two parameters are calculated over the last 100 bins of the spectrum similar to [5]

How to select n_σ?

- Tradeoff between reduction in error due to rejection of spurious spectral noise and increase in error due to reduced CNR and altered skew.
- Optimal value of n_σ for CW lidar depends on the spectral width [18].
- We choose an $n_\sigma = 5$, which conservatively eliminates noise outliers [16].

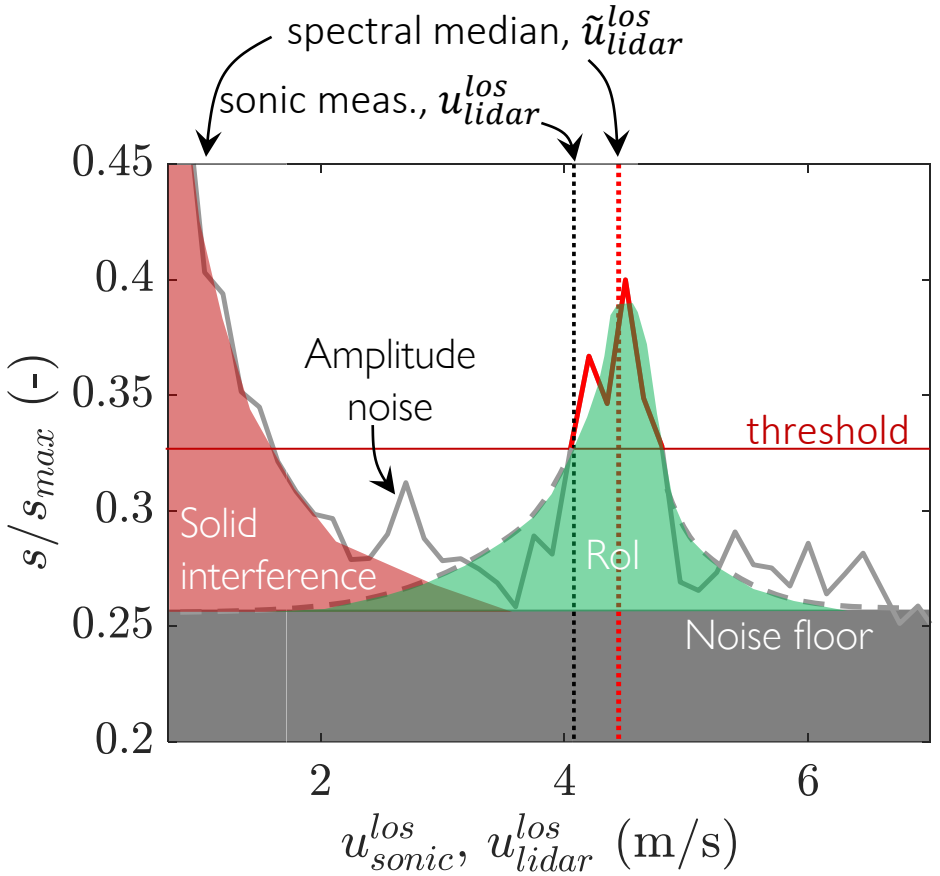

(CT technique only returns an estimate for cases as above that does NOT feature prominent solid interference)

Retrieval Techniques

Technique 2: advanced filtering (AF) [20]

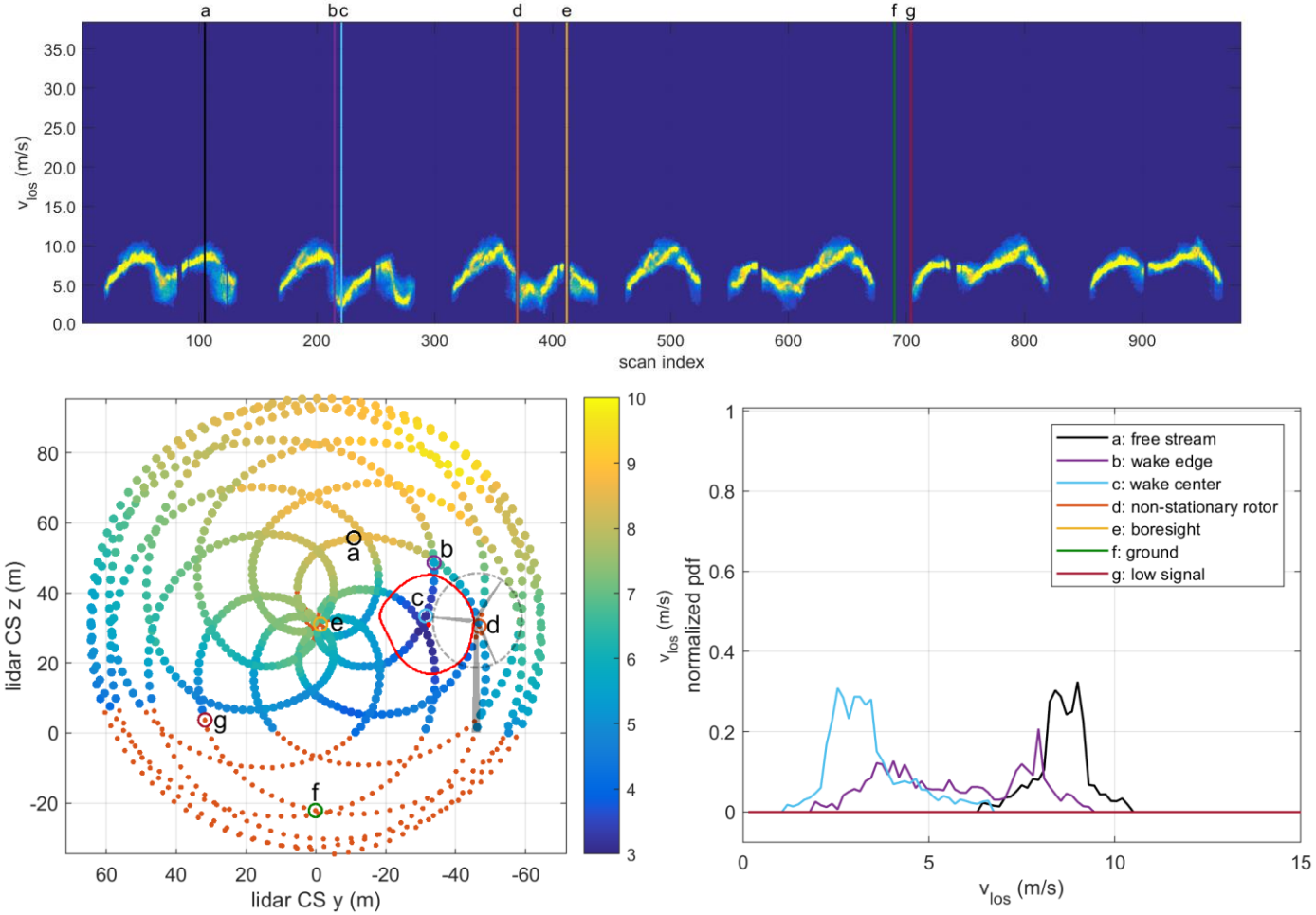

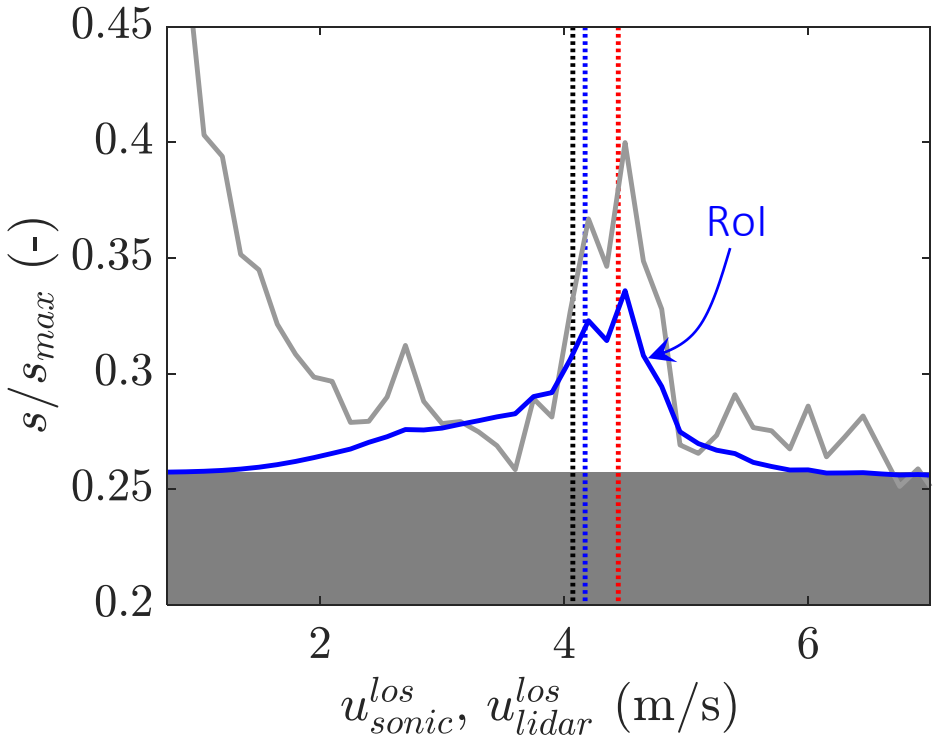

Retrieval Techniques

Technique 3: supervised machine learning regression (ML)

Testing:

- Range of test cases matches observed range of single-peaked returns in terms of CNR, median velocity, standard deviation, skew, and two parameters related to solid interference signature (exception: lower bound of median velocity is set at 2 m/s)
- Estimates are rejected if they have low confidence as calculated from the variance of the outputs from 32 networks
- ~13,000 test cases

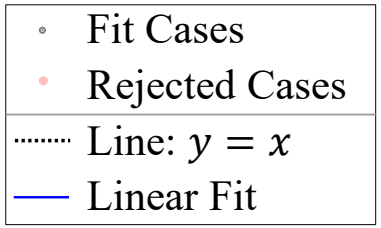

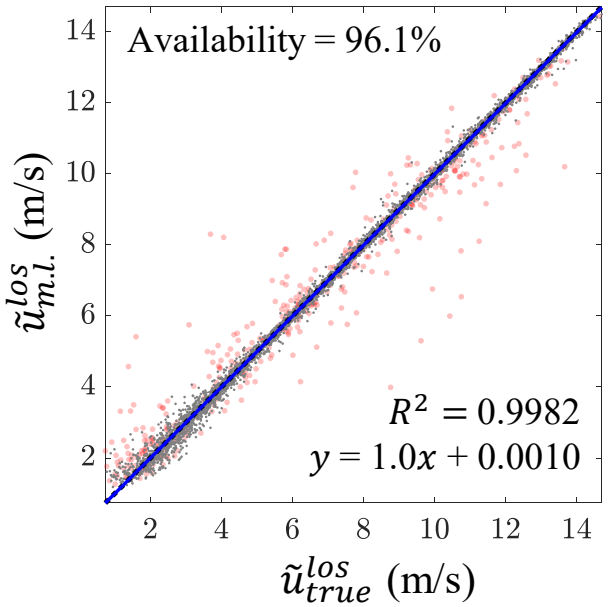

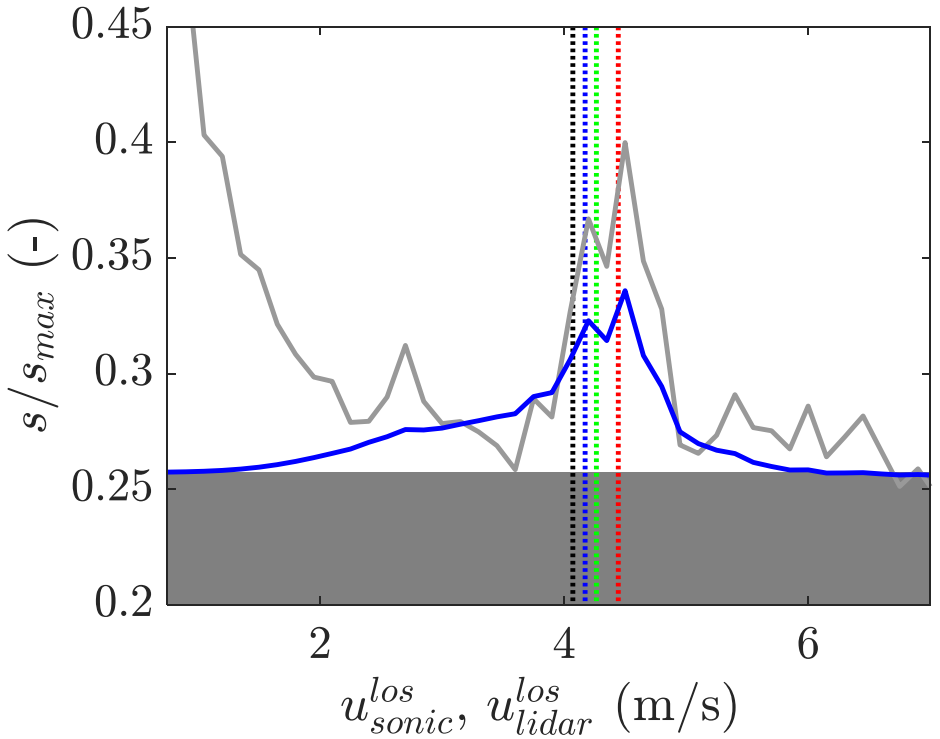

Results

Example case

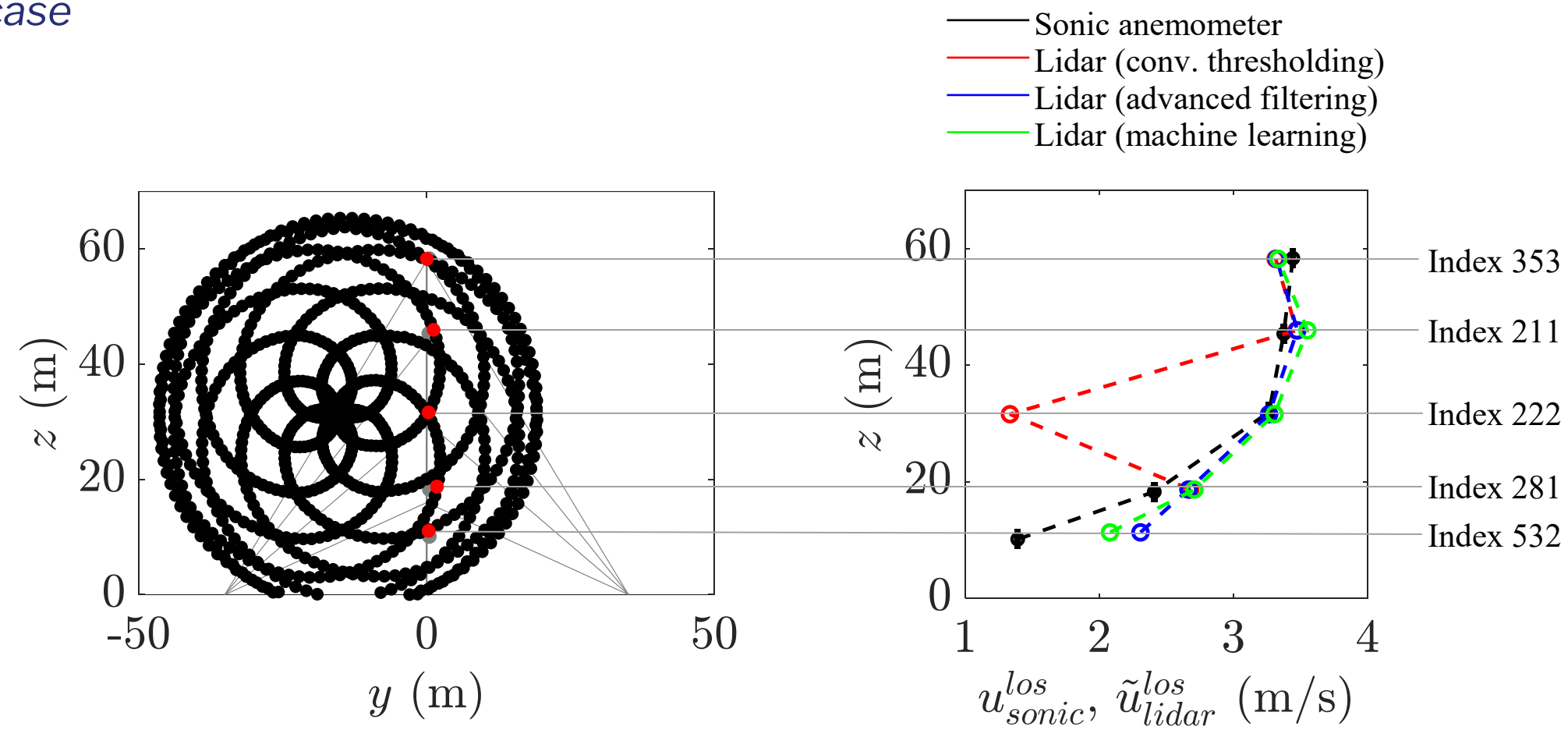

- Velocity estimates of the sonic anemometer indicate a roughly logarithmic boundary layer profile
- Disagreements between u^{los}_{sonic} and $\tilde{u}^{los}_{lidar}$ are congruous with our understanding of the lidar measurement principles and processing

Results

Inflow cases: error trends without solid interference

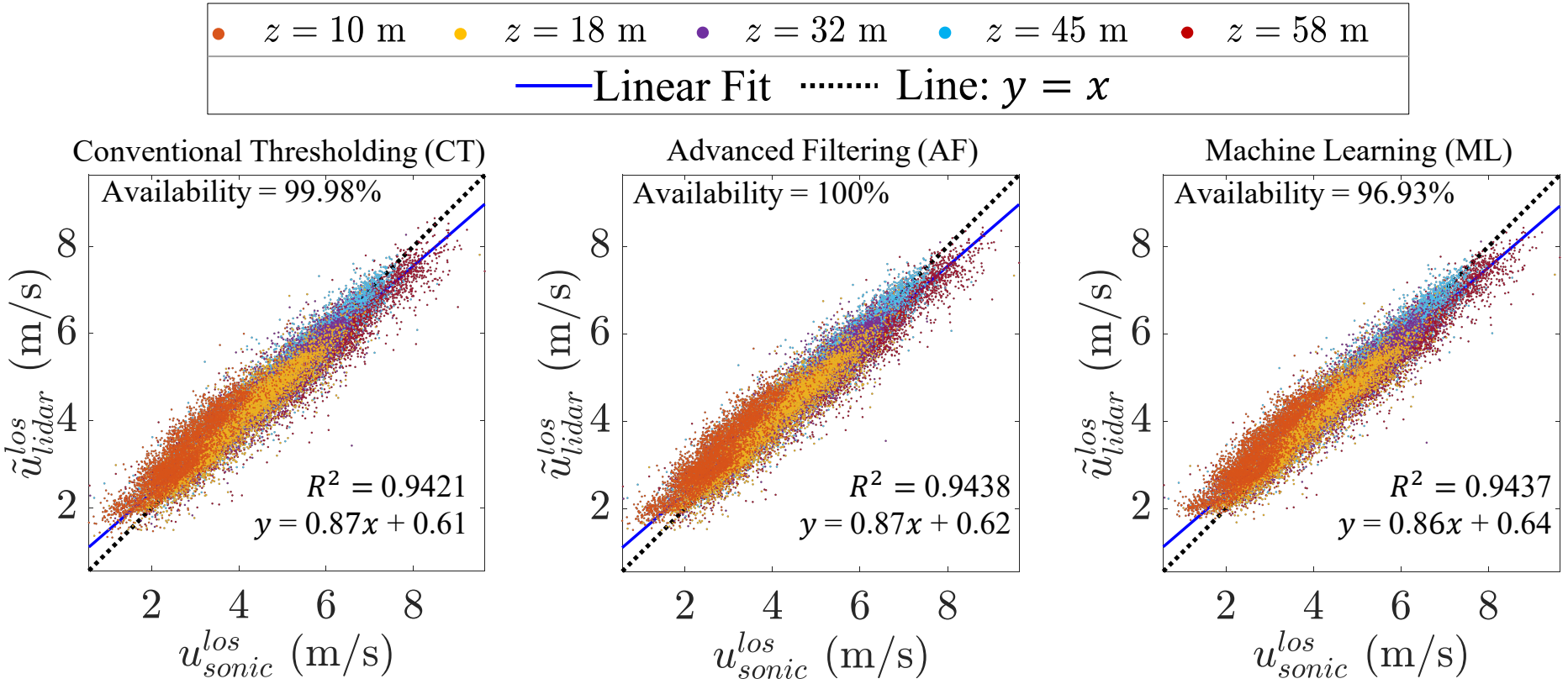

- Rather uninteresting comparison as hoped (i.e., all methods can handle clean returns)
- Residual errors: Bias → difference between the measurement volumes
  Scatter → difference between the measurement volumes and spectral noise

Results

Inflow cases: error trends without solid interference

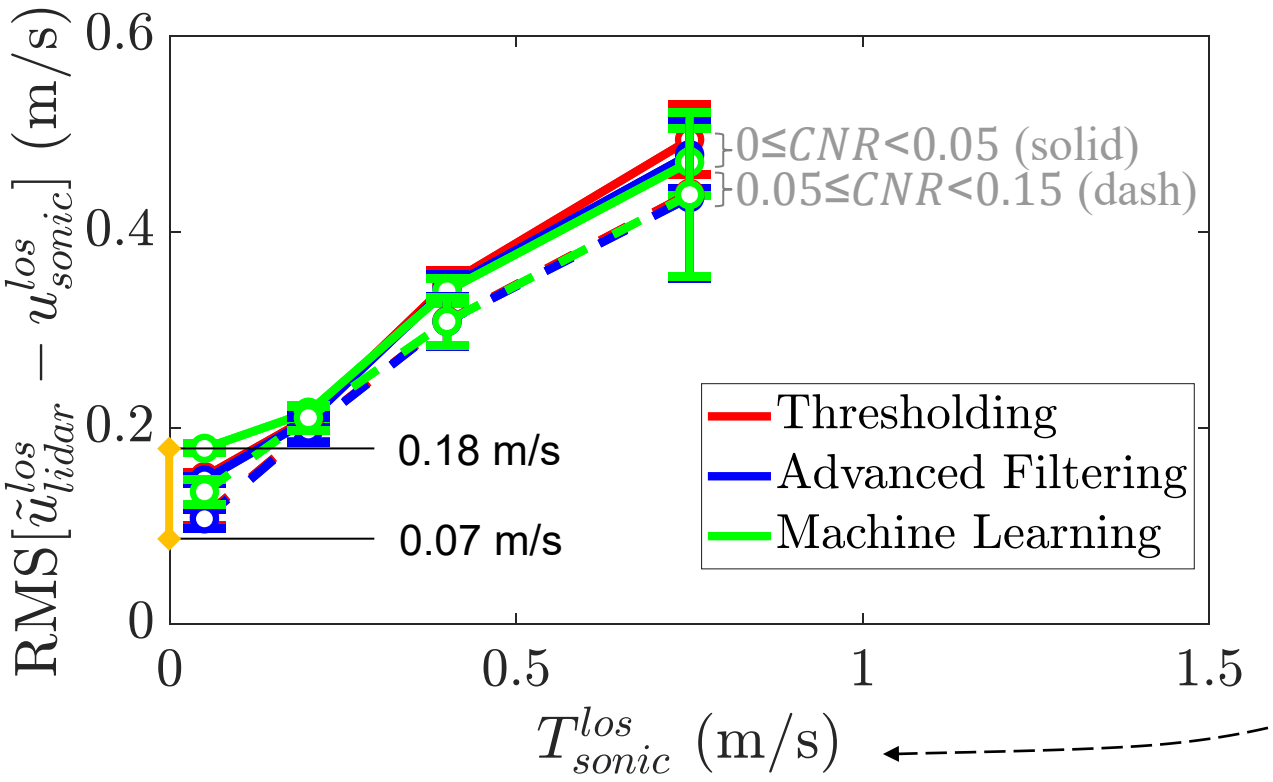

T_{sonic}^{los} is the running standard deviation of velocity from the sonic anemometer along the line-of-sight based on the filtering window

- Extrapolating the trend to zero turbulence gives a baseline uncertainty with RMS errors of roughly 0.07 to 0.18 m/s due to amplitude noise, and this is important information for model validation
- Little practical difference in spectral noise rejection exists between the three techniques

Results

Inflow cases: error trends with solid interference

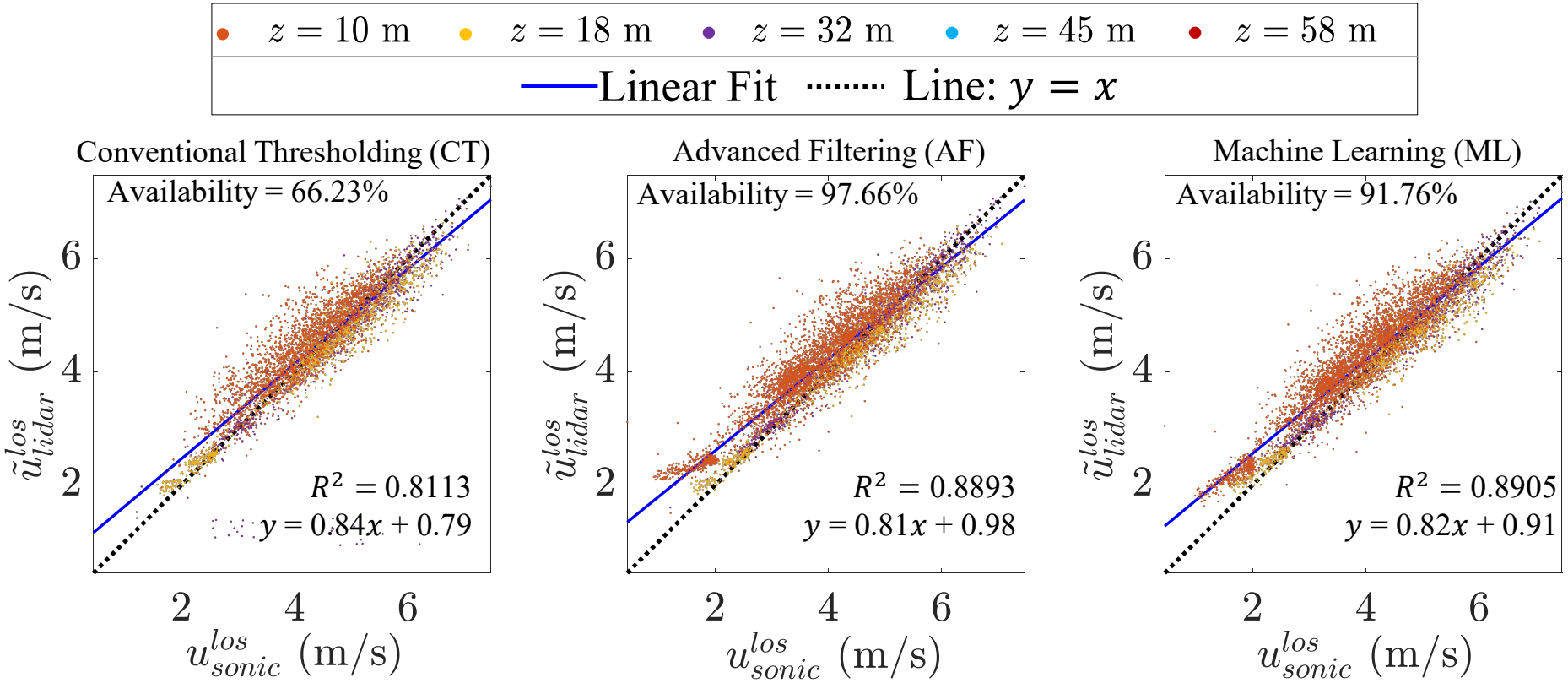

- Lower R^2 value of the CT technique primarily a consequence of a handful of partial solid returns that are not filtered out
- Between AF/ML, ML produces slightly lower scatter, which is traded for 5.9% lower data availability

Results

Inflow cases: practical significance

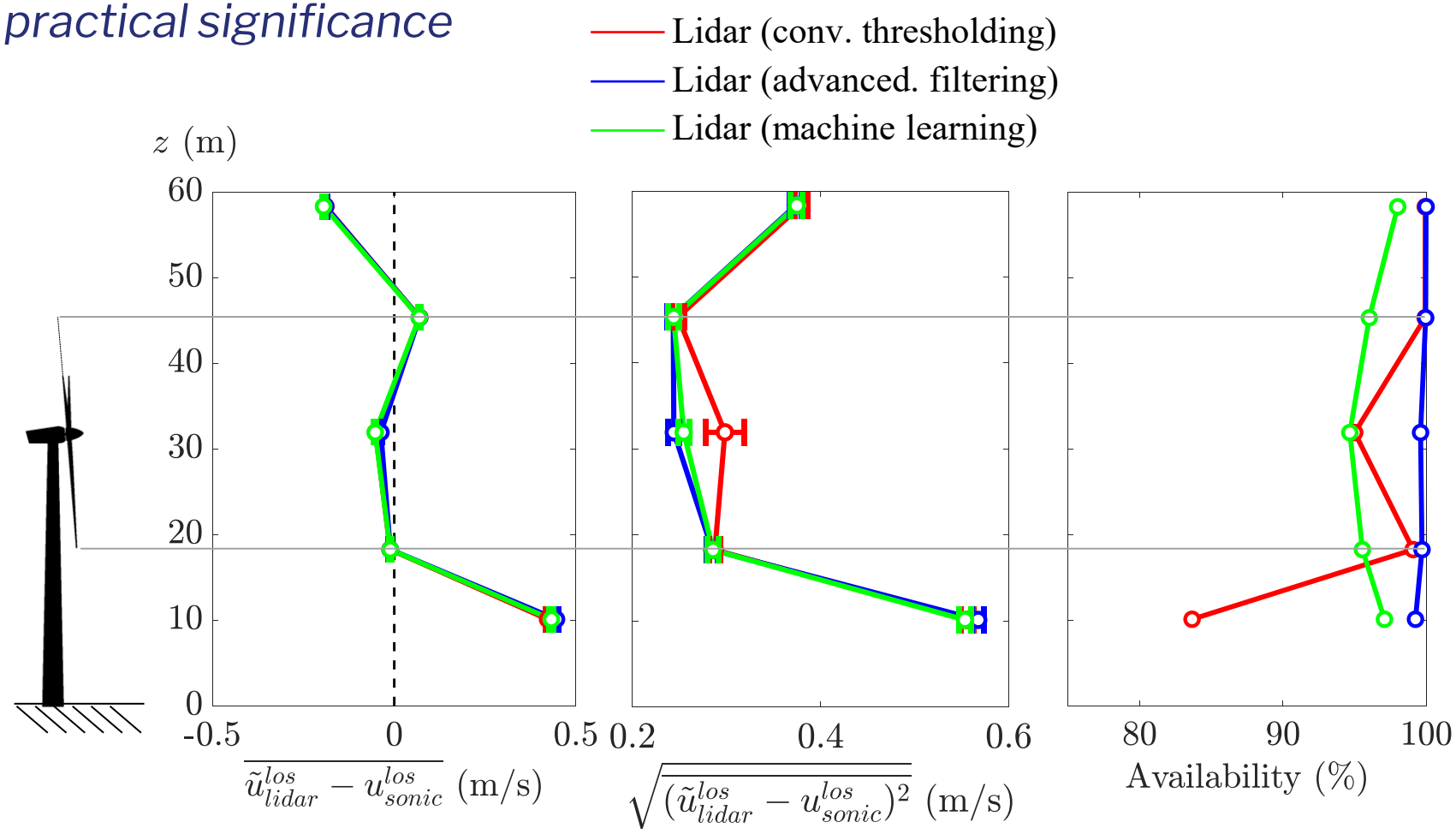

- RMS error is 0.2-0.3 m/s within the rotor height
- CT technique has 3-20% higher values within the rotor height depending on scan position because of its poor handling of solid returns

Results

Waked cases: practical significance

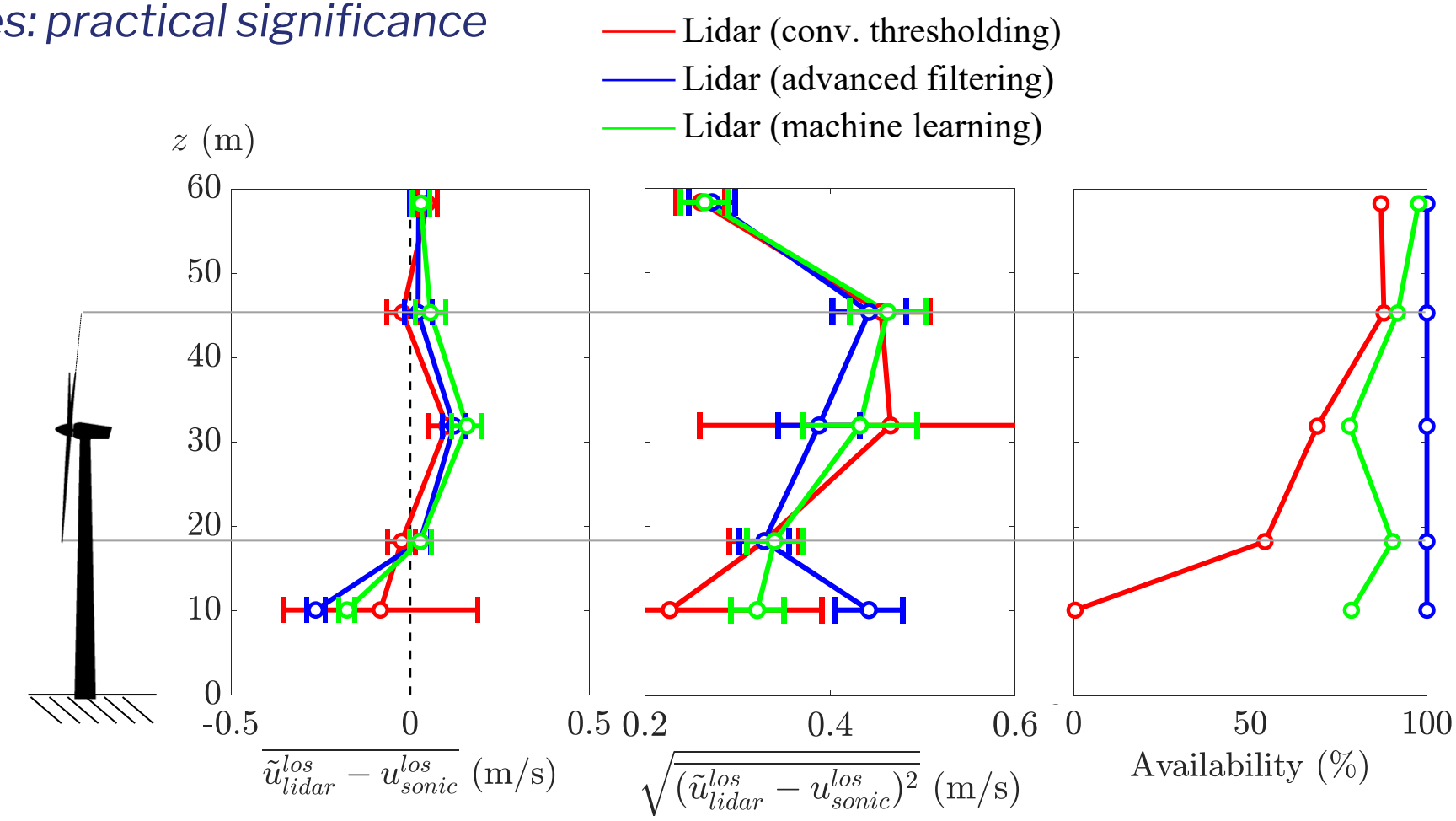

- Broad findings remain the same for the waked flow as for the inflow
- RMS error is now on the order of 0.3 to 0.5 m/s within the rotor height
- Ranking of proficiency of the three processing techniques is again (1) AF, (2) ML, (3) CT

Conclusions

- All three lidar processing techniques can produce similar performance when no solid interference is present
- AF and ML approaches generally give better performance than the CT when solid interference is present
  - → other sources of non-aerosol returns besides ground and meteorological tower: the optical window (i.e., boresight interference), nearby turbines, precipitation, and clouds
- AF technique (which was used for the Data Archive and Portal) is currently the best approach with RMS errors between 0.2-0.3 m/s for inflow cases and 0.3-0.5 m/s for wake cases
  - → results provide citable UQ for the 2016-2017 and future SWiFT campaigns
  - → results provide instrument error for SpinnerLidar to be used in upcoming campaigns
  - → results help improve experimental design (i.e., instrument selection + positioning)
  - → results guide future development of lidar retrieval techniques (CW and pulsed lidar)
- Although AF technique has performance advantage over ML, but the potential for improvement of the machine learning technique may be higher
  - → the machine learning approach therefore removes the ongoing expert commitment to the retrieval problem, instead shifting workload to a computer

References

1. Clifton, A., D. Elliott, and M. Courtney, *Ground-Based vertically profiling remote sensing for wind resource assessment*. 2013, Tech. Rep. 15, Internation Energy Agency.
2. Hasager, C., et al., *Hub height ocean winds over the North Sea observed by the NORSEWInD lidar array: measuring techniques, quality control and data management.* Remote Sensing, 2013. **5**(9): p. 4280-4303.
3. Mikkelsen, T., et al., *A spinner-integrated wind lidar for enhanced wind turbine control.* Wind Energy, 2013. **16**(4): p. 625-643.
4. Harris, M., M. Hand, and A. Wright, *Lidar for turbine control.* National Renewable Energy Laboratory, Golden, CO, Report No. NREL/TP-500-39154, 2006.
5. Simley, E., et al., *Analysis of light detection and ranging wind speed measurements for wind turbine control.* Wind Energy, 2014. **17**(3): p. 413-433.
6. Simley, E., et al., *Optimizing Lidars for wind turbine control applications—Results from the IEA wind task 32 Workshop.* Remote Sensing, 2018. **10**(6): p. 863.
7. Doubrawa, P., et al., *Multimodel validation of single wakes in neutral and stratified atmospheric conditions.* Wind Energy, 2020.
8. Hsieh, A.S., Brown, K.A., deVelder, N.B., Herges, T.G., Knaus, R.C., Sakievich, P.J., Cheung, L.C., Houchens, B.C., Blaylock, M.L., and Maniaci, D.C., *High-Fidelity Wind Farm Simulation Methodology with Experimental Validation.* Journal of Wind Engineering and Industrial Aerodynamics, 2021. **218**.
9. Lindelöw-Marsden, P. and D. Upwind, *Uncertainties in wind assessment with LIDAR.* Risø-R-1681UpWind Deliverable D1, 2009.
10. van Dooren, M.F., *Doppler Lidar Inflow Measurements.* Handbook of Wind Energy Aerodynamics, 2020: p. 1-34.
11. Herges, T.G., et al., *Scanning Lidar Spatial Calibration and Alignment Method for Wind Turbine Wake Characterization*, in *35th Wind Energy Symposium*. 2017.
12. Stawiarski, C., et al., *Scopes and Challenges of Dual-Doppler Lidar Wind Measurements—An Error Analysis.* Journal of Atmospheric and Oceanic Technology, 2013. **30**(9): p. 2044-2062.
13. Wang, H., et al., *Lidar arc scan uncertainty reduction through scanning geometry optimization.* Atmospheric Measurement Techniques, 2016. **9**(4): p. 1653-1669.
14. Forsting, A.R.M., N. Troldborg, and A. Borraccino, *Modelling lidar volume-averaging and its significance to wind turbine wake measurements.* Journal of Physics: Conference Series, 2017. **854**.
15. Sekar, A.P.K., et al. *How much flow information can a turbine-mounted lidar capture?* in *Journal of Physics: Conference Series*. 2020. IOP Publishing.
16. Peña, A. and C. Bay Hasager, *Remote sensing for wind energy.* 2013.
17. Liu, Z., et al., *Estimating random errors due to shot noise in backscatter lidar observations.* Applied optics, 2006. **45**(18): p. 4437-4447.
18. Angelou, N., et al. *Challenges in noise removal from Doppler spectra acquired by a continuous-wave lidar*. in *Proc. of the 26th Int. Laser Radar Conf., Porto Heli, Greece*. 2012.
19. Godwin, K., S. De Wekker, and G. Emmitt, *Retrieving winds in the surface layer over land using an airborne Doppler lidar.* Journal of Atmospheric and Oceanic Technology, 2012. **29**(4): p. 487-499.
20. Herges, T. and P. Keyantuo. *Robust Lidar Data Processing and Quality Control Methods Developed for the SWiFT Wake Steering Experiment*. in *Journal of Physics: Conference Series*. 2019. IOP Publishing.
21. Courtney, M., R. Wagner, and P. Lindelöw, *Testing and comparison of lidars for profile and turbulence measurements in wind energy.* IOP Conference Series: Earth and Environmental Science, 2008. **1**.
22. *Atmosphere to Elections (A2e) Data Archive and Portal*. 2019, U.S. Department of Energy, Office of Energy Efficiency and Renewable Energy.

Backup Slides

Generation of Synthetic Spectra

Two-step process to generate synthetic database

1. Collect data on lidar spectral return shapes from a broad range of field data

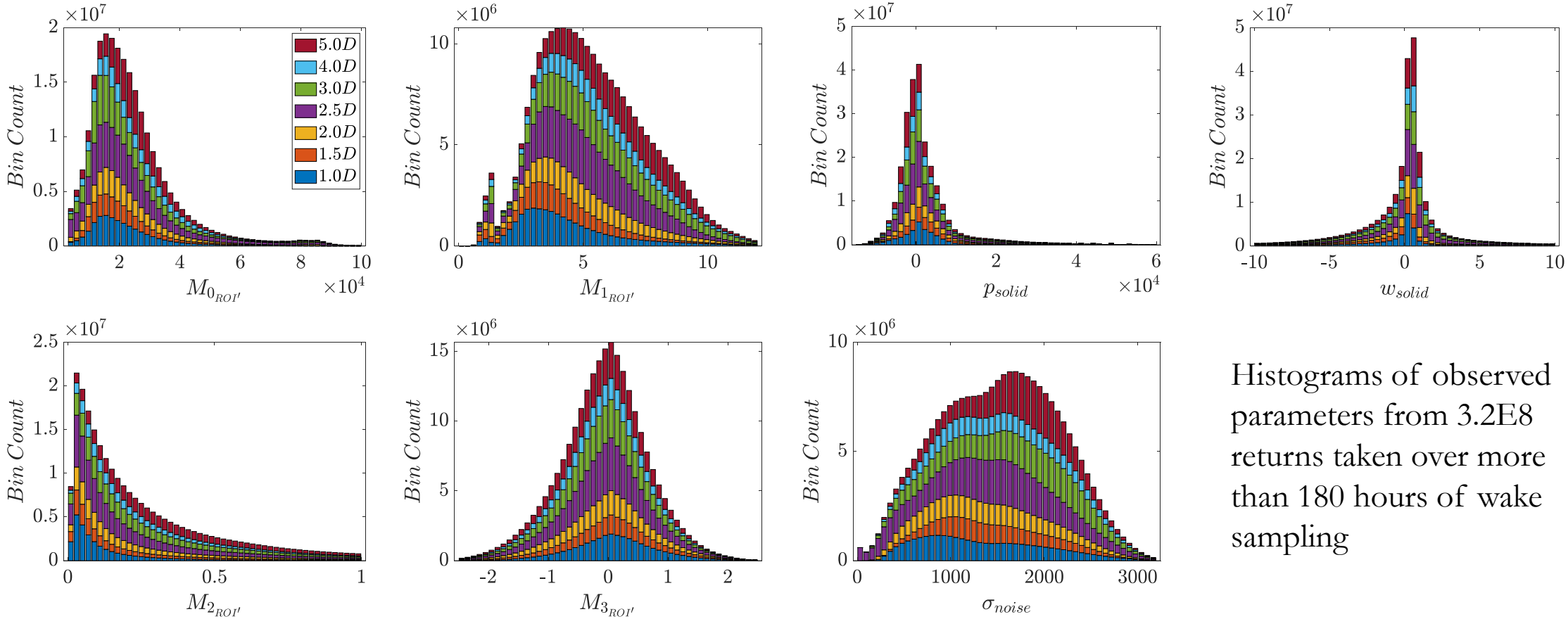

Histograms of observed parameters from 3.2E8 returns taken over more than 180 hours of wake sampling

Generation of Synthetic Spectra

Two-step process to generate synthetic database

2. Generate a database of synthetic lidar spectra with known ground truth quantities of interest (QoIs) and artificial contamination

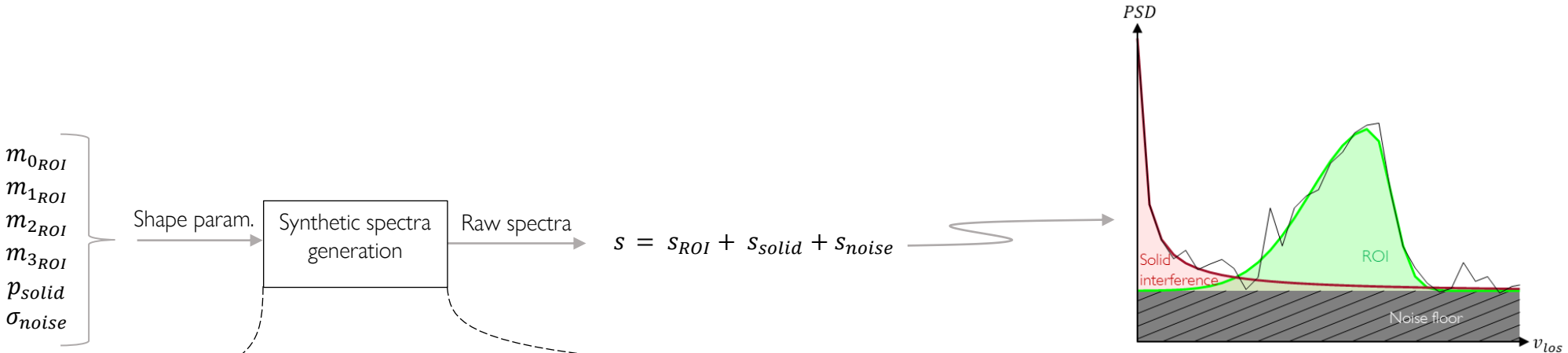

Scaled epsilon-skew-normal distribution [26]:

$$s_{ROI} = \frac{m_{0_{ROI}}}{m_{2_{ROI}}\sqrt{2\pi}} e^{-\frac{1}{2}\left(\frac{v_{los}-m_{1_{ROI}}}{m_{2_{ROI}}(1\mp m_{3_{ROI}})}\right)^2}$$

Inverse function:

$$s_{solid} = \frac{p_{solid}}{1+(v_{los}-v_{solid})/w_{solid}}$$

Randomized instances of noise (>400 per case):

$$s_{noise} = normrnd(0, \sigma_{noise}) \quad \text{for each bin}$$

26. Mudholkar, G.S. and A.D. Hutson, *The epsilon–skew–normal distribution for analyzing near-normal data.* Journal of statistical planning and inference, 2000. **83**(2): p. 291-309.